Bone Reports 7 (2017) 17–25

Contents lists available at ScienceDirect

Bone Reports

journal homepage: www.elsevier.com/locate/bonr

Mechanical instability and titanium particles induce similar transcriptomic changes in a rat model for periprosthetic osteolysis and aseptic loosening

Mehdi Amirhosseini[a,*], Göran Andersson[b], Per Aspenberg[c], Anna Fahlgren[a]

[a] Division of Cell Biology, Department of Clinical and Experimental Medicine, Faculty of Medicine and Health Sciences, Linköping University, Linköping, Sweden
[b] Division of Pathology, Department of Laboratory Medicine, Karolinska Institutet, Karolinska University Hospital, Huddinge, Sweden
[c] Orthopedics, Department of Clinical and Experimental Medicine, Faculty of Medicine and Health Sciences, Linköping University, Linköping, Sweden

ARTICLE INFO

Keywords:
Aseptic loosening
Implant
Instability
Wear debris
Microarray

ABSTRACT

Wear debris particles released from prosthetic bearing surfaces and mechanical instability of implants are two main causes of periprosthetic osteolysis. While particle-induced loosening has been studied extensively, mechanisms through which mechanical factors lead to implant loosening have been less investigated. This study compares the transcriptional profiles associated with osteolysis in a rat model for aseptic loosening, induced by either mechanical instability or titanium particles. Rats were exposed to mechanical instability or titanium particles. After 15 min, 3, 48 or 120 h from start of the stimulation, gene expression changes in periprosthetic bone tissue was determined by microarray analysis. Microarray data were analyzed by PANTHER Gene List Analysis tool and Ingenuity Pathway Analysis (IPA). Both types of osteolytic stimulation led to gene regulation in comparison to unstimulated controls after 3, 48 or 120 h. However, when mechanical instability was compared to titanium particles, no gene showed a statistically significant difference (fold change $\geq \pm 1.5$ and adjusted p-value ≤ 0.05) at any time point. There was a remarkable similarity in numbers and functional classification of regulated genes. Pathway analysis showed several inflammatory pathways activated by both stimuli, including Acute Phase Response signaling, IL-6 signaling and Oncostatin M signaling. Quantitative PCR confirmed the changes in expression of key genes involved in osteolysis observed by global transcriptomics. Inflammatory mediators including interleukin (IL)-6, IL-1β, chemokine (C-C motif) ligand (CCL)2, prostaglandin-endoperoxide synthase (Ptgs)2 and leukemia inhibitory factor (LIF) showed strong upregulation, as assessed by both microarray and qPCR. By investigating genome-wide expression changes we show that, despite the different nature of mechanical implant instability and titanium particles, osteolysis seems to be induced through similar biological and signaling pathways in this rat model for aseptic loosening. Pathways associated to the innate inflammatory response appear to be a major driver for osteolysis. Our findings implicate early restriction of inflammation to be critical to prevent or mitigate osteolysis and aseptic loosening of orthopedic implants.

1. Introduction

Despite a high success rate for hip and knee arthroplasty, the number of patients in need of revision is estimated to increase as a result of long-term implant failure (Kurtz et al., 2007) primarily due to aseptic loosening (Ulrich et al., 2008; Aujla and Esler, 2017). Bisphosphonates and TNF (Tumor necrosis factor)-blockers have been tested to alleviate ongoing bone resorption at the bone-implant interface and the consequent implant loosening, but failed to prove effective. Only when given intraoperatively, bisphosphonates seem to prevent resorption and early loosening (Schilcher et al., 2017). For established loosening, surgical intervention is thus the only option to restore function after aseptic loosening of orthopedic implants.

In the tissue surrounding loosened prostheses, the osteoclast-osteoblast balance is disrupted in favor of bone-resorbing osteoclasts. Higher ratios of osteoclast/osteoblast numbers have been observed in bone tissue from patients with osteolysis around loosened compared to well-fixed prostheses (Kadoya et al., 1996). In the tissue surrounding loosened implants, TNF (Xu et al., 1996), IL (Interleukin)-1β (Kim et al., 1993), IL-6 (Sabokbar and Rushton, 1995), CCL (Chemokine (C-C motif) ligand) 2 and CCL3 (Nakashima et al., 1999) and other mediators are present. Macrophage activating marker CHIT-1 (Chitinase 1), and IL-8, as well as osteoclast differentiation and function markers like DC-STAMP (Dendritic cell-specific transmembrane protein), TRAP (Tartrate-resistant acid phosphatase) and Cathepsin K were found elevated in periprosthetic tissue of loosened implants (Koulouvaris et al., 2008).

* Corresponding author.
E-mail addresses: mehdi.amirhosseini@liu.se (M. Amirhosseini), goran.andersson@ki.se (G. Andersson), per.aspenberg@liu.se (P. Aspenberg), anna.fahlgren@liu.se (A. Fahlgren).

http://dx.doi.org/10.1016/j.bonr.2017.07.003
Received 15 December 2016; Received in revised form 24 July 2017; Accepted 26 July 2017
Available online 29 July 2017

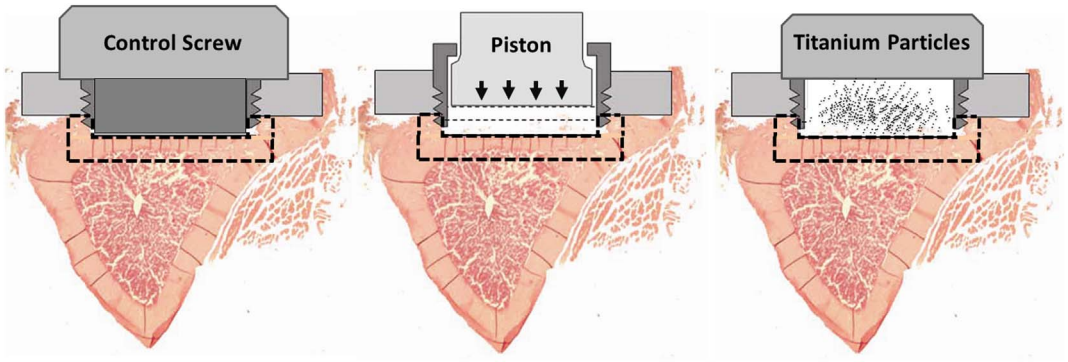

Fig. 1. Validated rat model for aseptic loosening. The animal model allows for application of particles, representing wear debris particles, or simulation of mechanical instability corresponding to implant micromotion. The marked area indicates where samples were harvested for RNA isolation.

In aseptically failed total knee arthroplasty (TKA) and total hip arthroplasty (THA), differences in CCL3, NFκB (Nuclear factor kappa-B ligand) and DC-STAMP levels were found between TKA and THA, suggesting that different mechanisms might underlie bone degradation and aseptic loosening depending on location of implant (Tomankova et al., 2014).

Bone resorption induced by wear debris particles is well characterized. A foreign body response, mediated primarily through phagocytic activity of macrophages, plays a key role along with a plethora of inflammatory cytokines and chemokines contributing to the immune reaction and recruitment of inflammatory cells to the site (Ingham and Fisher, 2005; Veronesi et al., 2017). Inflammatory mediators elevate RANKL levels which is a crucial osteoclastogenesis inducer (Ingham and Fisher, 2005). In macrophage cultures, exposure to particles induces several inflammatory mediators, known to promote osteoclast differentiation (Horowitz and Gonzales, 1997; Garrigues et al., 2005). The number and function of osteoblasts is also reported to be negatively affected by different types of particles (Lochner et al., 2011; Queally et al., 2009; Atkins et al., 2009). Moreover, human mesenchymal stem cells have shown lower survival rate (Wang et al., 2002) and blunted osteogenic differentiation capacity (Okafor et al., 2006) after exposure to titanium particles.

Apart from wear debris from prosthetic surfaces, mechanical factors like instability of implants leading to micromotion may induce fluid pressure changes resulting in fluid flow, which has been associated with aseptic loosening (Gallo et al., 2013; Sundfeldt et al., 2006). Clinical case studies have linked fluid flow (Anthony et al., 1990) and fluid pressure (Walter et al., 2004; Robertsson et al., 1997) to osteolytic lesions around orthopedic prostheses. Substantial increases in RANKL/OPG (Osteoprotegerin) ratio mRNA levels have been reported following ex vivo loading of human bone cores mimicking the mechanical condition at bone-implant interfaces (Stadelmann et al., 2008). Studies in animal models for aseptic loosening have highlighted the role of implant micromotion and fluctuating fluid flow in periprosthetic bone resorption (Aspenberg and Herbertsson, 1996; van der Vis et al., 1998; Van der Vis et al., 1999; Skripitz and Aspenberg, 2000; Jones et al., 2001; Skoglund and Aspenberg, 2003; Fahlgren et al., 2010). We previously (Nilsson et al., 2012) reported that, in a clinically relevant rat model for aseptic loosening (Skripitz and Aspenberg, 2000; Fahlgren et al., 2010), titanium particles and mechanical instability of implants induced a similar extent of osteoclast differentiation assessed by immunohistochemistry and osteoclast numbers. Although periprosthetic osteolysis induced by particles has been investigated extensively, biological mechanisms through which mechanical instability leads to osteolysis are not fully clarified. Here, for the first time, we compared the in vivo gene expression patterns following exposure to either mechanical instability or titanium particles through global transcriptome profiling in our validated animal model for aseptic loosening.

2. Materials and methods

2.1. Animal model

This study was approved by Linköping animal experiments ethical committee (ethical # 85-12) and all experiments were carried out in accordance to guidelines for care and treatment of experimental animals recommended by the committee. In total, 66 male 11-week-old Sprague-Dawley rats, weighing approximately 370 g (SD = 17) at the start of the experiments, were used. Two rats were housed in each ventilated cage in 12-hour light/dark cycle with access to food and water ad libitum. A validated animal model for aseptic loosening, described in detail previously (Skripitz and Aspenberg, 2000; Fahlgren et al., 2010), was used to either induce mechanical instability or administer titanium particles.

Briefly, following general anesthesia induced by 5% isoflurane and preoperative subcutaneous injection of 20 mg/kg Engemycin and 7 mg/kg Carprofen, the top surface of the cortical bone on the right proximal tibia was milled down and a titanium plate was fixed on the bone and left to osseointegrate. The plate had a central plug that could be removed to allow access to the bone surface. After 5 weeks of osseointegration a second surgery, with preoperative subcutaneous injections of 20 mg/kg Engemycin and 0.04 mg/kg Temgesic was performed. And the plug was removed and replaced with either an instability piston to induce mechanical instability corresponding to implant micromotion, or a hollow screw containing titanium particles to simulate wear debris particles released from prosthetic surfaces (Fig. 1).

With the instability piston in place, there was a 1-mm space between the piston and the bone. By pressing on the piston manually through the skin, it could be moved 0.5 mm down to pressurize the fluid in the 1-mm space. This creates a flow propagating through and along the underlying bone. The instability piston does not reach the bone surface during instability episodes (a 0.5-mm gap remains), avoiding risk of microfractures. To induce mechanical instability, 20 displacement cycles with a force of 8 N at 0.17 Hz, during 2 min (Fahlgren et al., 2010), were applied twice a day under anesthesia. Control animals underwent the same surgery and the central plug was removed from their implants before sample collection but they were not administered particles or implant displacement.

The moving parts of the piston are isolated from the bone by a silicone membrane, and previous histological evaluations of bone tissue under the implant have shown that induction of mechanical instability does not release any debris particles from implant surfaces (Skripitz and Aspenberg, 2000; Fahlgren et al., 2010; Nilsson et al., 2012). When harvesting, samples from groups exposed to titanium particles were evaluated macroscopically, confirming that particles were spread over the bone surface. All animals were in good health throughout the experiments period and no signs of infection were observed at any time.

Table 1
Number of animals/group used for microarray and qPCR analysis at each time point.

Group	n[a] (microarray)	n (qPCR)
Control	4	6
Ti 3 h	4	6
Ti 48 h	3	5
Ti 120 h	3	5
Me 3 h	4	7
Me 48 h	3	6
Me 120 h	3	6
Control (15 min)	4	7
Ti 15 min	4	8
Me 15 min	4	8

Ti: titanium particles; Me: mechanical instability.
[a] From each group of animals (n = 5–8), 3–4 samples were chosen for microarray analysis based on the quality of RNA.

2.2. Study design

The animals were randomized into groups of controls, titanium particles and mechanical instability (Table 1). Rats exposed to titanium particles or mechanical instability were further divided into three different follow-up time groups and were euthanized 3 h, 48 h and 120 h after the start of the stimulation. Transcriptome analysis was performed at 3 time points to assess the inflammatory response and regulation of transcription factors (3 h) recruitment of precursor cells and osteoclast differentiation (48 h) and osteoclast maturation and function (120h). In an additional experiment, to explore possible differences in the earliest gene expression changes caused by instability and particles, the same procedure was repeated in a new set of animals. The rats were randomized into groups of control, titanium particles and mechanical instability and euthanized 15 min after stimulation.

Immediately after euthanasia using CO_2 gas, the bone tissue under the implant was harvested using a trephine with an internal diameter of 4.5 mm. The harvested bone tissue from under the implants has previously been confirmed to undergo osteolysis after 5 days of exposure to titanium particle or instability (Fahlgren et al., 2010; Nilsson et al., 2012). The harvested bone tissue was rinsed with cold saline, and the underlying bone marrow was carefully removed from the bone specimens. No periosteum was present as the implants were osseointegrated. Two rats were excluded due to technical problems during sample harvest. Samples were immediately snap-frozen in liquid nitrogen and kept at − 80 °C before RNA isolation and quality control prior to microarray analysis. The study design is summarized in a flow chart (Fig. 2).

2.3. Preparation of titanium particles

Pure titanium and titanium alloy particles are the most frequently used type of particles to investigate gene expression changes in particle-induced osteolysis although with a large variability in size range (0.1–20 μm) and concentration (Veronesi et al., 2017). Here commercially pure titanium particles (Alfa Aesar, Karlsruhe, Germany) with 93% of the particles < 20 μm and 90% of them < 3.6 μm in size were used (Nilsson et al., 2012). Particles were suspended in 95% ethanol for 30 min and subsequently heated at 200 °C for 3 h and confirmed to be LPS (Lipopolysaccharide)-free by *Limulus Amebocyte Lysate* (LAL) assay for endotoxin (Pierce, IL, USA). Using normal saline, a 400 mg/ml particle suspension was prepared under sterile conditions and sonicated for 10 min. The particle stock was vortexed vigorously just before use and a volume of 10 μl, enough to cover the bone surface, was placed inside the hollow screws and applied adjacent to the bone tissue under the implants. No particles were administered to the mechanical instability groups.

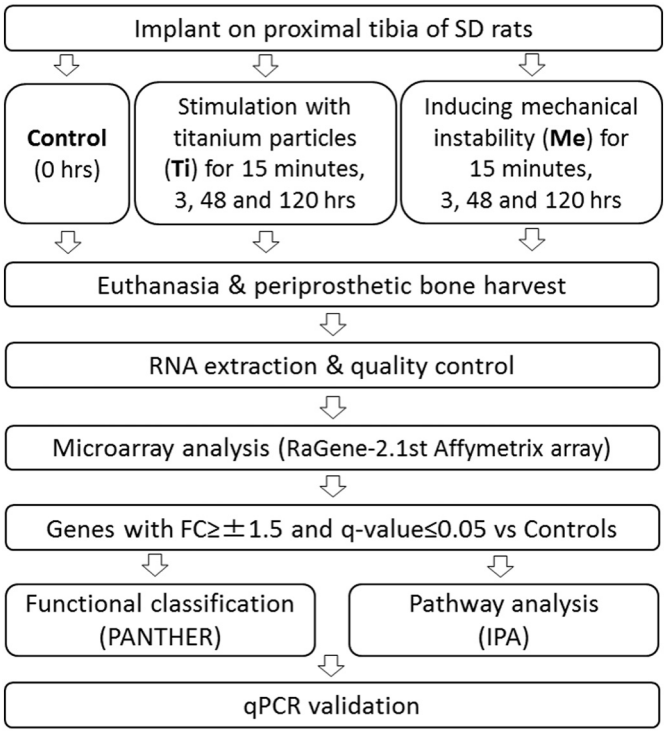

Fig. 2. Flow chart describing the work flow and study design.

2.4. Sample homogenization and RNA isolation

A combination of TRIzol method and RNeasy Mini Kit (QIAGEN, Sollentuna, Sweden) were used to isolate RNA from bone samples (Reno et al., 1997). Frozen bone samples were pulverized by tungsten balls, inside vials cooled by liquid Nitrogen, in a Retsch mixer mill MM 200 (Retsch, Haan, Germany). Samples were kept frozen during the whole homogenization procedure. Immediately after pulverization, TRIzol (Invitrogen) was added to samples and left to thaw at room temperature. Next, chloroform wad added followed by centrifugation and the aqueous phase was then transferred to new tubes and mixed gently with 70% ethanol. RNA samples were purified according to the RNeasy Mini Kit instructions. RNase-free DNase Set (QIAGEN, Sollentuna, Sweden) was used to exclude possible DNA contamination. Quality of RNA samples including concentration and RIN (RNA Integrity Number) value were checked by Nanodrop ND-1000 (NanoDrop Technologies, Wilmington, DE) and Agilent RNA 6000 Nano Kit (Agilent Technologies, Böblingen, Germany). Samples were kept at − 80 °C before microarray analysis.

2.5. Microarray hybridization and data normalization

RNA samples (n = 3–4/group) chosen based on RNA integrity number (RIN) were analyzed using RaGene-2.1-st array (Affymetrix, Santa Clara, CA). The microarray hybridization and normalization of raw data were performed using Affymetrix Expression Console (method: med-polish (rma-bg, quant-norm, sketch = − 1, bioc = true, lowprecision = false, usepm = true, target = 0, doavg = false)) by the Bioinformatics and Expression Analysis (BEA) core facility at the Karolinska Institute. Fold changes were calculated from the mean of log2-transformed data and p-values generated by Student's *t*-test were FDR (false discovery rate)-adjusted (q-values).

2.6. Microarray data analysis and differentially expressed genes

Genes with a minimum fold change of ± 1.5 compared to unstimulated controls and q-value ≤ 0.05 were considered differentially

expressed and used for further analysis. PANTHER classification tool (Mi et al., 2013) was used for functional classification of regulated genes and QIAGEN's Ingenuity® Pathway Analysis (IPA®, QIAGEN Redwood City, *www.qiagen.com/ingenuity*) was used to analyze molecular and cellular functions and regulated pathways. GeneSpring was used for hierarchical clustering and principal component analysis (PCA).

After applying the cut-off for fold change and q-value, if the number of regulated genes was > 1000, only the top 1000 genes with the highest fold change were uploaded to IPA for analysis. Comparison analysis in IPA was performed to contrast data analysis outputs from mechanical instability and titanium particles against each other. Pathways with activation z-score ≥ ± 2 and p-value < 0.05 determined by IPA were considered significantly regulated. When filtering microarray data based on fold change and q-value, in cases where no significantly changed genes were detected, a less strict filtering criteria (FC ≥ ± 1.2 and q-value ≤ 0.1) was also tested to determine type II errors.

2.7. Quantitative real time polymerase chain reaction

To validate our findings from microarray, RNA samples (n = 5–8/group) were converted to cDNA using High Capacity cDNA Reverse Transcription Kit (Applied Biosystems) and qPCR was carried out using standard curve methodology. Selection of genes was based on their role in osteoclast differentiation and function and the fold change detected in the data from microarray. Primers (Applied Biosystems) for IL-1α (Rn00566700_m1), IL-1β (Rn00580432_m1), IL-6 (Rn01410330_m1), CCL2 (Rn00580555_m1), Ptgs2 (Rn01483828_m1), LIF (Rn00573491_g1), CD14 (Rn00572656_g1), Csf1 (Rn01522726_m1), RANKL (Rn00589289_m1), OPG (Rn00563499_m1), Acp5 (Rn00569608_m1) and Ctsk (Rn00580723_m1) were used and amplification was performed in duplicate using TaqMan Fast PCR Master mix (Applied Biosystems). Expression levels in samples were normalized to beta-2 microglobulin (Rn00560865_m1) which was expressed steadily between groups.

2.8. Statistics

The qPCR data were analyzed by Kruskal-Wallis test. Differences induced by each stimulus compared to the controls as well as difference between mechanical instability versus titanium particles at each time point were determined by Mann-Whitney *U* test. A p-value < 0.05 was considered statistically significant.

3. Results

3.1. Temporal dynamics of transcriptional activity during osteolysis

Similar numbers of genes were differentially regulated at 3, 48 and 120 h by mechanical instability compared to controls (344, 1909 and 973) and titanium particles (302, 1884 and 864) compared to controls, after filtering microarray data based on minimum fold change of ± 1.5 and q-value ≤ 0.05 (Fig. 3A,B). When mechanical instability and titanium particles were compared, there were no genes with a statistically significant difference at any time point (Fig. 3C). A cut-off of fold change ≥ ± 1.2 and q-value ≤ 0.1 did not change this pattern.

The distribution of differentially expressed genes induced by mechanical instability or titanium particles compared to unstimulated controls over time was then depicted in Venn diagrams. Of all differentially regulated genes, both stimuli showed a similar distribution over time (Fig. S1). Hierarchical clustering of the samples indicated similar gene expression patterns between mechanical instability and titanium particles, particularly at 3 h, with a distinct change in clustering of up- and down-regulated genes at 48 and 120 h compared to samples at 3 h and controls (Fig. S2A). The principal component analysis (PCA) also visualized clustering of the samples by time point rather than by treatment (Fig. S2B). Top 10 up- and down-regulated genes by titanium particles and mechanical instability with highest fold change at 3, 48 and 120 h are presented in Supplementary materials (Tables S1A,B).

3.2. Functional classification of regulated genes

Genes regulated by mechanical instability and titanium particles versus controls after 3, 48 and 120 h showed apparent similarity in function. Almost the same proportion of genes involved in different biofunctions were induced by the two stimuli; including “cellular process”, “apoptotic process”, “immune system process”, “biological adhesion”, “localization” and “response to stimulus” among others (Fig. 4; Table S2). The same similarity was found when the top 5 molecular and cellular functions and the correlated number of genes were analyzed over time and treatment using IPA (Table S3).

3.3. Pathway analysis

A wide range of inflammatory pathways associated to osteolysis were regulated by mechanical instability and titanium particles at all time points. These include Acute Phase Response signaling, IL-6 signaling, Oncostatin M signaling and HMGB1 (High mobility group-B1) signaling among others (Fig. 5). Differences in the regulated pathways within treatments at different time points were noticeable. Initially, it appeared that there were differences between some pathways regulated by instability and particles (e.g. Oncostatin M signaling at 48 h, IL-6 signaling at 120 h). However, after comparing fold changes and significance levels of genes regulating each pathway, it was evident that in all cases the difference was due to fold changes and/or q-values that override our cut-off point only slightly, and consequently were filtered out; therefore they were not considered true differences.

Apart from ongoing inflammatory responses at all time points, a simplified classification showed that pathways involved in regulation of cell death and survival were notable at 3 h; processes involved in cell proliferation and differentiation were prominent at 3 and 48 h; and pathways related to cytoskeletal reorganization, cell adhesion and migration were predominant at 120 h (Fig. 5). Categories and top functions of regulated signaling pathways by instability and particles are presented in the Supplementary materials (Table S4).

3.4. Regulation of genes associated to osteolysis and osteogenesis

According to the microarray data, there was no significant

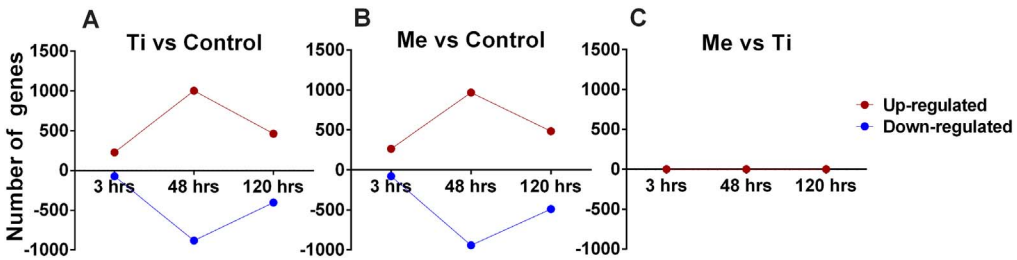

Fig. 3. Number of differentially regulated genes by each stimuli. Regulated genes by titanium particles (Ti) and mechanical instability (Me) with fold change ≥ ± 1.5 and q-value ≤ 0.05, after 3, 48 and 120 h compared to unstimulated controls. A) Titanium particles versus controls; B) Mechanical instability versus controls; C) Mechanical instability versus titanium particles.

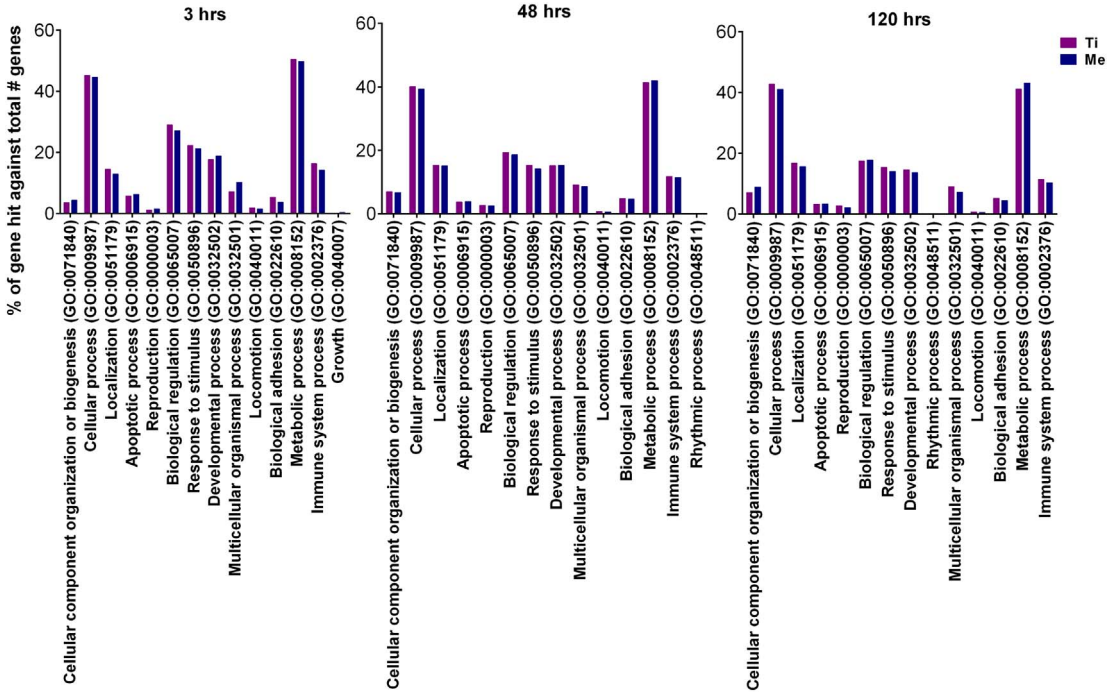

Fig. 4. Functional classification of regulated genes. Comparison of functional classification of differentially regulated genes (FC ≥ ± 1.5 and q-value ≤ 0.05) by titanium particles (Ti) and mechanical instability (Me) after 3, 48 and 120 h, using PANTHER Gene List Analysis tool, indicating the percentage of genes involved in different functions.

difference between the two stimuli regarding genes known to be involved in osteoclast and osteoblast differentiation and function. Transcription factors like FOS (FBJ osteosarcoma oncogene) and NFκB1 showed the highest levels at 3 h and matrix metalloproteinases at 120 h. Most inflammatory mediators, including IL-6, IL-1β, CCL2, Oncostatin M, LIF (Leukemia inhibitory factor) and Ptgs2 (Prostaglandin-endoperoxide synthase 2), showed their peak levels at 3 h. The up-regulation of monocyte/macrophage markers CD14 and Csf1 (Colony stimulating factor 1) started at 3 h while CD68, MSR1 (Macrophage scavenger receptor 1) and CD11b were up-regulated at later time points. Genes involved in osteoblast differentiation and bone formation were predominantly down-regulated. Bglap, BMP-4 and BMP-7 were decreased at 48 and 120 h compared to controls while BMP-2 was up-regulated at 3 h. Runx2 showed highest levels at 48 h while ALP started to elevate at 48 h and remained up-regulated at 120 h. Wnt (Wingless-related integration site) signaling agonists, like Wnt5a, Wnt16, Fzd (Frizzled family receptor) 1 and Fzd2, showed highest levels at 48 h while Wnt signaling inhibitors such as Sclerostin, Dkk1 (Dickkopf Wnt signaling pathway inhibitor 1) and Sfrp2 (Secreted frizzled-related protein 2) were down-regulated. A table with fold changes and statistical significance levels induced by instability and particles compared to unstimulated controls based on microarray analysis is available in the Supplementary materials (Table S5).

3.5. Microarray analysis at 15 min

Despite the entirely different nature of these two osteolytic stimuli, a remarkable similarity between gene expression patterns induced by instability and particles was observed after 3, 48 and 120 h. We speculated that differences between responses to mechanical instability and titanium particles lie in the initiation stage of the osteolytic process; hence could be detected at an earlier time point. We repeated the experiments and assessed data from samples harvested 15 min after stimulation and found no differentially regulated genes compared to controls based on a minimum fold change of ± 1.5 and q-value cut-off of 0.05. A filtering criterion of fold change ≥ ± 1.2 and q-value ≤ 0.1 showed the same pattern.

Although at 15 min we did not detect any genes differentially regulated based on the q-value threshold, genes with fold change above ± 1.2 and (unadjusted) p-value < 0.05 (307 genes for mechanical instability and 994 genes for titanium particles) were assessed for functional classification and the similarity between mechanical instability and particles was again evident (Fig. S3).

3.6. qPCR validation

Validation of expression changes in 12 key genes involved in osteoclast differentiation and function by qPCR, revealed the same pattern as observed in the microarray data. Comparing the fold difference and relative changes by the two stimuli in the analyzed genes detected by qPCR and microarray (Table 2) showed a substantial overlap.

After 3 h, inflammatory mediators were up-regulated by both particles and instability with their peak levels at 3 h. Similar to our microarray findings, the most substantial changes were observed in IL-6 levels at 3 h, with 100-fold ($p = 0.02$) and 185-fold ($p = 0.01$) increase by titanium particles and mechanical instability respectively (Fig. 6A) as well as in Ptgs2 which was also remarkably increased after 3 h (Ti: 28-fold, $p = 0.01$; Me: 37-fold, $p = 0.01$) (Fig. 6D). A significant difference was found between IL-6 levels induced by titanium particles and mechanical instability at 48 h ($p = 0.02$) as well as in Ptgs2 levels at 120 h ($p = 0.01$).

IL-1β mRNA levels showed a significant rise after 3 h induced by both stimuli (Ti: 4.3-fold, $p = 0.01$; Me: 5.6-fold, $p = 0.01$) in comparison to controls but declined at later time points (Fig. 6B). CCL2 and LIF were up-regulated in response to both particles and instability at 3, 48 and 120 h although with a descending pattern over time (Fig. 6E,F). IL-1α was increased by both stimuli with no significant difference between them (Fig. 6C).

Monocyte/macrophage markers CD14 and Csf1 both showed rapid up-regulation induced by particles and instability at 3 h with CD14 remaining significantly high at 48 and 120 h (Fig. 6G,H). A significant difference between Csf1 mRNA levels induced by titanium particles (1.7-fold vs controls) and mechanical instability (2.4-fold vs controls) at 3 h was detected.

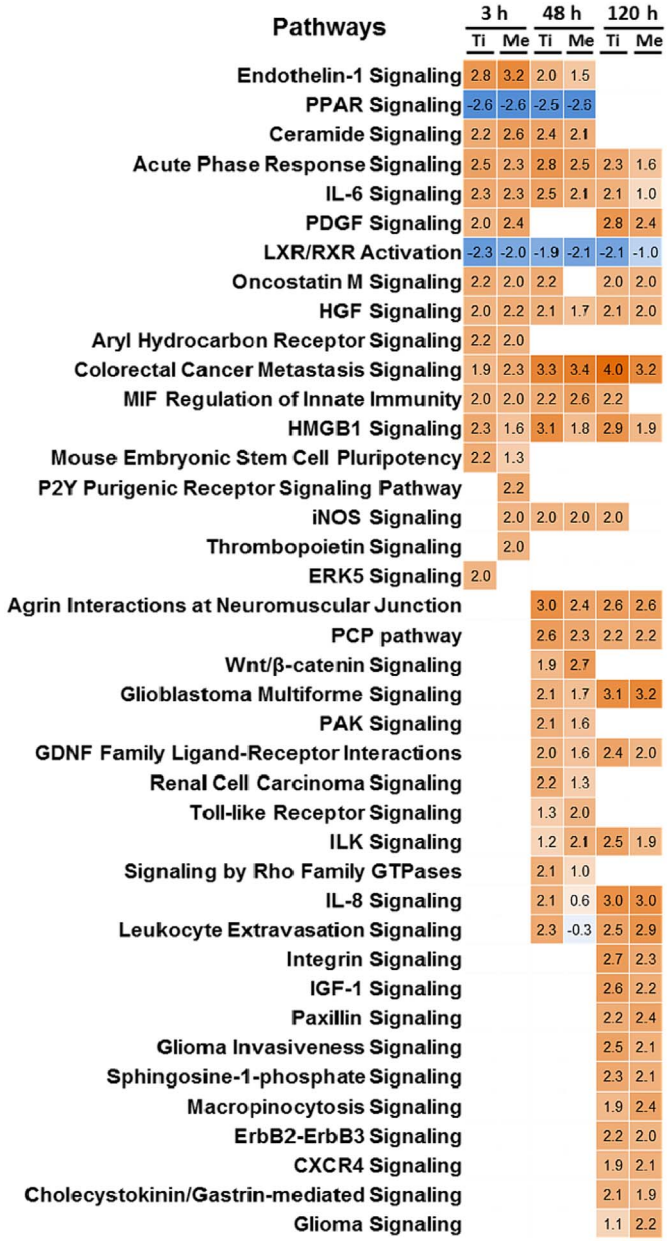

Fig. 5. Comparison analysis of regulated pathways. Heatmap of pathways regulated by titanium particles (Ti) and mechanical instability (Me) after 3, 48 and 120 h. Numbers on the heatmap indicate activation z-scores. Pathways with z-score ≥ ± 2 and a p-value cut-off of $-log10$ of 1.3 were considered significantly regulated in the comparison analysis by IPA. CXCR4: Chemokine (C-X-C motif) Receptor-4, ERK5: Extracellular signal regulated kinase 5, GDNF: Glial cell-derived neurotrophic factor, HGF: Hepatocyte growth factor, HMGB1: High mobility group-B1, IGF-1: Insulin-like growth factor-1, IL-6: Interleukin 6, IL-8: Interleukin 8, ILK: Integrin-linked kinase, iNOS: Nitric oxide synthase 2 (inducible), LXR/RXR: Liver X receptor/Retinoid X receptor, MIF: Macrophage migration inhibitory factor, PAK: p21 activated protein kinases, PCP: Planar cell polarity, PDGF: Platelet-derived growth factor, PPAR: Peroxisome proliferator-activated receptor.

Regarding genes involved in osteoclast differentiation and activity, RANKL mRNA levels peaked at 48 h in response to both stimuli (Ti: 6.5-fold, p = 0.01; Me: 4.7-fold, p = 0.01) remaining significantly elevated until 120 h (Fig. 6I). OPG expression on the other hand was increased already after 3 h by both particles (4.2-fold, p = 0.01) and instability (8.9-fold, p = 0.01). While OPG mRNA levels were still significantly elevated in response to mechanical instability (5.2-fold, p = 0.02), at 48 h they declined with titanium particles (1.7-fold, p = 0.07) (Fig. 6J).

TRAP mRNA did not show any significant changes (Fig. 6K) while Cathepsin K, a more selective marker for osteoclasts, was up-regulated by titanium particles (2.2-fold, p = 0.01) after 48 h and by both stimuli at 120 h (Ti: 2-fold, p = 0.04; Me: 2.3-fold, p = 0.01) (Fig. 6L).

Our analyses by qPCR showed that after 15 min 10 out of 12 investigated genes were not significantly regulated by particles or instability (Fig. S4). However, Ptgs2 (2.2-fold, p = 0.01) and IL-1β (1.8-fold, p = 0.01) mRNA were up-regulated significantly compared to controls by mechanical instability but not by titanium particles (Fig. 7A,B). The change in Ptgs2 mRNA levels induced by mechanical instability was also significant compared to that of titanium particles (p = 0.04) (Fig. 7A).

Table 2
Comparison of fold changes induced by titanium particles (Ti) and mechanical instability (Me) compared to controls detected by qPCR (n = 5–8/group) and microarray (n = 3–4/group).

Gene	Method	Ti 3	Me 3	Ti 48	Me 48	Ti 120	Me 120
IL-6	qPCR	99.7†	185†	27†	9.8†	2.7	6.1†
	Microarray	74.6*	75.3*	26.2*	7*	3.7*	9.6
IL-1β	qPCR	4.3†	5.6†	1.6	1.4	0.97	2.9
	Microarray	3.7*	3.5	1.17	1.02	1.1	4.1
IL-1α	qPCR	2.9†	5.6†	2.3†	1.4	1.5†	9†
	Microarray	2.9*	4.2	2*	0.99	1.4	11.7
Ptgs2	qPCR	28.3†	37.2†	6†	7.3†	1.8†	6.6†
	Microarray	18.6*	17.1	5*	5.9*	2.1*	7.4
CCL2	qPCR	9.7†	15.9†	5.6†	3.8†	3.2†	2.9†
	Microarray	6.9*	7.1*	5.4*	3.5*	3.3	3.7*
LIF	qPCR	5.2†	11.6†	4.6†	2.9†	2.6†	3.2†
	Microarray	5.5*	6.4	5.4*	2.5*	2.7*	4.1*
CD14	qPCR	4.1†	4.7†	2.6†	4.3†	1.9†	2.4†
	Microarray	3.5*	3.4*	2.6*	3.4*	2*	2.9
Csf1	qPCR	1.7†	2.4†	1.6	2	1.3	1.6†
	Microarray	2.1	2.2*	1.9*	2*	1.6*	2*
RANKL	qPCR	1.3	1.9†	6.5†	4.7†	2.6†	4.2†
	Microarray	1.3	1.3	5.8*	3.5*	2.5*	4.6
OPG	qPCR	4.2†	8.9†	1.7	5.2†	1.5	1.7
	Microarray	2.6*	3.8*	1.8*	3.4*	1.5	1.4
Ctsk	qPCR	0.7	1.02	2.2†	1.2	2†	2.3†
	Microarray	0.91	0.98	1.3*	0.99	1.2	1.3*

CCL2: Chemokine (C-C motif) ligand 2, CD14: CD14 molecule, Csf1: Colony stimulating factor 1 (macrophage), Ctsk: Cathepsin K, IL-1α: Interleukin 1 alpha, IL-1β: Interleukin 1 beta, IL-6: Interleukin 6, LIF: Leukemia inhibitory factor, OPG: Osteoprotegerin, Ptgs2: Prostaglandin-endoperoxide synthase 2, RANKL: Receptor activator of nuclear factor κ B ligand

* q-Value < 0.05.

† p-Value < 0.05.

4. Discussion

This is the first in vivo study comparing gene expression profiles during osteolysis induced by mechanical instability and titanium particles separately. We previously observed that titanium particles and mechanical instability induced similar rates of osteoclast differentiation in our validated animal model for aseptic loosening (Nilsson et al., 2012). Here we examined the transcriptome changes in bone tissue exposed to either mechanical instability or titanium particles for different time periods and found that already 3 h after each individual stimulus, there were similar biological processes and signaling pathways involved.

The similar gene expression patterns caused by the two stimuli after 3, 48 and 120 h, became apparent after an overall assessment of the microarray data. Most notably, comparison of differentially regulated genes by mechanical instability versus titanium particles did not identify any genes with statistically significant difference in expression between instability and particles.

Changes in certain modulated signaling pathways suggest a role of an innate immune response in the course of aseptic loosening induced by implant instability. Microarray as well as confirmatory qPCR analysis indicated increased expression of several inflammatory mediators

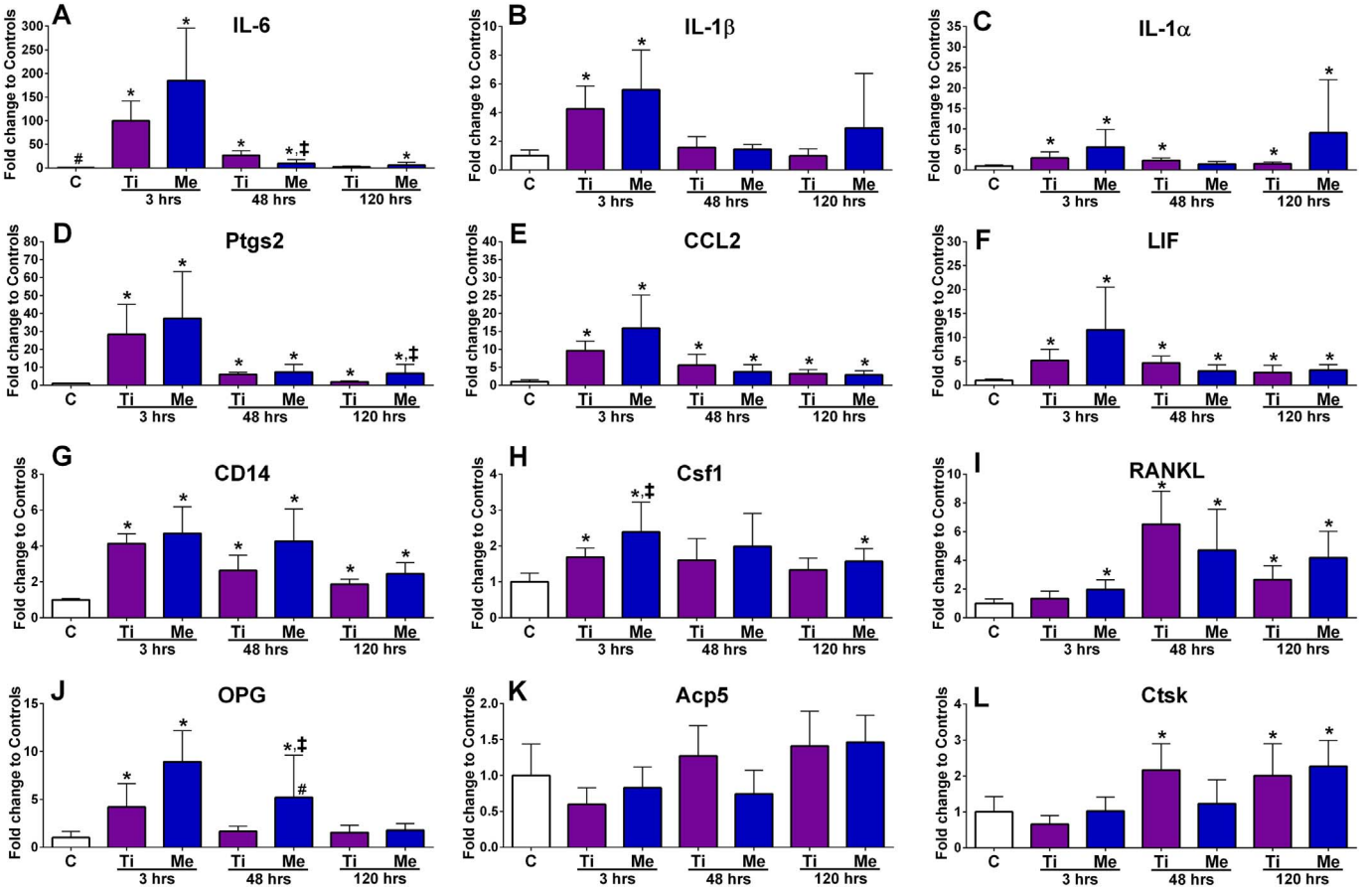

Fig. 6. mRNA expression changes following exposure to titanium particles (Ti) or mechanical instability (Me) at 3, 48 and 120 h investigated by qPCR. *: Significantly different from controls ($p < 0.05$). ‡: Significant difference between mechanical instability and titanium particles ($p < 0.05$). #: Samples with Ct value > 35 were excluded.

induced by both stimuli. As a general pattern, the inflammatory response was strongest at 3 h, although it persisted until 120 h.

The role of the IL-6 family of cytokines in osteoclast differentiation has been highlighted previously (Sims and Walsh, 2010). IL-6 and LIF mRNA levels were elevated by both particles and instability as investigated by qPCR, and IL-6 has been linked to increased RANKL/OPG ratio levels (Sims and Walsh, 2010). Overexpression of IL-6 in transgenic mice increases osteoclastogenesis and dampens osteoblast function (De Benedetti et al., 2006). The increase in expression of inflammatory mediators in our data is in agreement with our previous, less comprehensive findings, where iNOS, prostaglandin E synthase (PGES) and IL-6 were up-regulated after 24 h by both mechanical instability and titanium particles (Nilsson et al., 2012).

CD14 and Csf1 were up-regulated already at 3 h by both stimuli. This indicates a rapid activation of the monocyte/macrophage lineage within few hours of stimulation which in turn contributes to enhanced production of inflammatory cytokines.

Regarding osteoclastogenesis, RANKL mRNA expression displayed their peak levels at 48 h in both groups and remained high until 120 h. Although instability seemed to cause a faster rise in RANKL mRNA compared to controls, observed at 3 h, there was no significant difference between the two stimuli at any time point. Positive correlations between inflammatory cytokines and RANKL levels in patients with loosening of total hip arthroplasty have been reported (Wang et al., 2010). OPG showed the highest up-regulation at 3 h in both groups. OPG has been associated to cell survival and prevention of apoptosis (Weinstein et al., 2011; Chamoux et al., 2008; Holen and Shipman, 2006). On the other hand, pro-inflammatory effects by OPG (Nahidi et al., 2013) and induction of OPG in response to inflammatory cytokines (De Voogd et al., 2016; Pantouli et al., 2005) have been reported. This has been suggested to have a modulatory role in restricting inflammation (De Voogd et al., 2016).

Our data suggest that titanium particles induced a faster osteoclastogenic response compared to mechanical instability. This can be

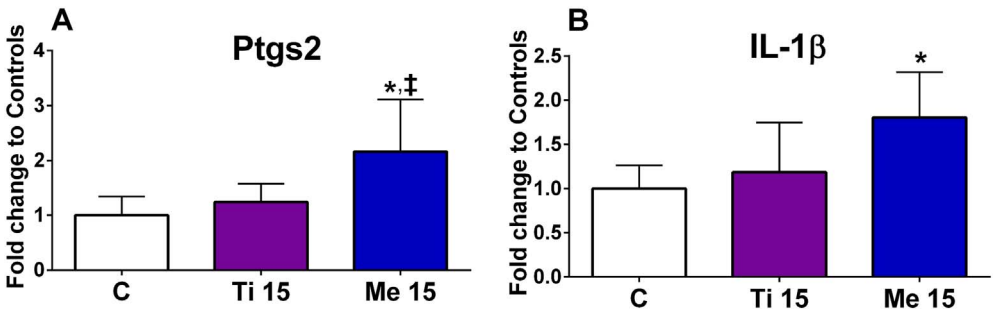

Fig. 7. mRNA expression changes 15 min after exposure to titanium particles (Ti) or mechanical instability (Me) investigated by qPCR. *: Significantly different from controls ($p < 0.05$). ‡: Significant difference between mechanical instability and titanium particles ($p < 0.05$).

observed in RANKL and OPG changes at 48 h where RANKL levels were higher with particles while instability induced higher OPG levels compared to particles. A similar pattern is evident with Cathepsin K which showed significant increase after 48 h with particles while both stimuli induced same increase rate at 120 h compared to controls. Similarly TRAP, although not showing any significant changes, was higher in the particle group at 48 h and exhibited similar levels at 120 h in both groups. The qPCR analysis indicated a clear pattern of early macrophage activation and cytokine production which could lead to regulation of osteoclastogenesis and osteolysis through changes in RANKL and Cathepsin K at later time points.

Microarray analysis after 15 min yielded no significant changes compared to unstimulated controls. However, confirmatory qPCR with more samples was done. No changes were detected by the two stimuli using qPCR either, except an up-regulation of Ptgs2 and IL-1β caused by mechanical instability compared to controls. Ptgs2 and IL-1β are both expressed by macrophages in association to mechanical forces. Preventing mechanical loading by joint immobilization was reported to reduce IL-1β levels in mice with osteoarthritis (Burleigh et al., 2012). Applying mechanical load on synovial-like membranes collected from the interface of aseptically failed total hip arthroplasties led to high IL-1β and prostaglandin E_2 expression (Bosetti et al., 2001). Induction of Ptgs2 by mechanical strains in MLO-Y4 cells (Govey et al., 2015; Liu et al., 2015) and human tendon fibroblasts (Yang et al., 2005) have been reported. The quick rise in mRNA levels of Ptgs2 and IL-1β triggered by instability implicates them as early responders to implant micromotion. This might be associated to the fact that a mechanical force is likely to spread through tissue and reach cells faster compared to particles. However, after 3 h both stimuli elicited similar mRNA levels of cytokines.

The role of the Wnt signaling pathway in bone remodeling has been studied broadly. The Wnt/β-catenin signaling pathway (48 h) and non-canonical Wnt-planar cell polarity (PCP) signaling pathway (48 and 120 h) were activated according to pathway analysis. Bone anabolic effects of Wnt/β-catenin signaling through enhanced osteoblastogenesis have been confirmed previously (Westendorf et al., 2004; Kim et al., 2013). However, Wnt signaling also affects osteoclast differentiation. Wnt/β-catenin signaling has been shown to inhibit osteoclastogenesis (Wei et al., 2011; Weivoda et al., 2016). On the other hand, non-canonical Wnt signaling, specifically Wnt5a, is reported to induce differentiation of osteoclasts (Weivoda et al., 2016; Maeda et al., 2012). Activation of both canonical and non-canonical Wnt signaling pathways observed here, suggests compensatory bone anabolic processes occurring in parallel to osteoclast differentiation in the periprosthetic tissue.

Cytoskeletal reorganization, starting at 48 h with ILK (Integrin-linked kinase) and PAK (p21 activated protein kinases) signaling, was most notable at 120 h. In order to resorb bone, osteoclasts need to adhere to and migrate along bone surfaces where cytoskeletal rearrangement is crucial. Integrins and Paxillin are adhesion proteins taking part in podosome formation in the sealing zone of osteoclasts (Novack and Faccio, 2011). Rho family GTPases signaling, activated at 48 h, was indicated to be involved in podosome formation/disruption in osteoclasts (Ory et al., 2008). Another cytoskeleton-dependent process regulated at 120 h is Macropinocytosis signaling, involved in endocytosis. However, it should be remembered that our data is derived from tissues comprising different cell types; therefore associating functions to specific cell populations should be done with caution.

The pivotal role of the innate immune response, particularly macrophages, has been carefully elucidated in aseptic loosening induced by particles (Nich and Goodman, 2014; Ren et al., 2011). The similar dependence on innate immunity between particle- and instability-induced mechanisms is further supported by our previous observation that the glucocorticoid agonist dexamethasone, an inhibitor of immune system and inflammation in general, blunted instability-induced resorption in the same model (Nilsson et al., 2012). These findings suggest that mechanical instability regulates aseptic loosening through inflammatory processes previously shown to be relevant for wear debris particles.

An inflammatory response following mechanical loading has been reported previously in a rat forelimb model where a transient activation of inflammatory pathways prior to the load-induced bone anabolic response was observed (McKenzie et al., 2011). However, in our animal model, a pathological condition induced by implant instability and micromotion led to a persistent inflammatory response similar to that caused by particles. Presumably, magnitude and duration determines how and to what extent inflammation affects bone structure.

The high number of genes regulated at later time points of our study makes analyzing and unfolding possible subtleties in the data complicated. Other factors regulating expression of genes like DNA methylation or histone modifications could also play roles, not assessed here. Another point is to be aware of the intricate issue of translating numbers and expression values of one or a set of genes into biological effects.

Most microarray data on the etiology of bone loss caused by particles or mechanical forces are generated from in vitro studies. The main downside of assessing cell cultures with a homogenous cell population is the absence of communication and signal transduction between different cell types as it occurs in the periprosthetic tissue. In this study, we used an animal model which was previously validated to induce similar rates of osteoclast differentiation with titanium particles and mechanical instability (Nilsson et al., 2012) giving us the opportunity to study and compare the gene expression changes caused by particles and instability of implants independently.

Given the different characteristics of the two stimuli, it could be speculated that the very first steps in the processes leading to periprosthetic osteolysis are different. Here, through qPCR, we detected increased levels of Ptgs2 and IL-1β caused by mechanical instability as early as 15 min after induction of implant micromotion. This suggests that mechanical stimulation is capable of eliciting a rapid inflammatory response. However, it appears that already few hours after induction of instability or exposure to particles, inflammatory processes ensue and act as the main driving force behind osteolysis in response to mechanical instability and titanium particles in our animal model. This might explain the difficulty to restrain aseptic loosening using anti-inflammatory drugs, since various inflammatory pathways and mediators seem to work simultaneously towards osteoclast differentiation. Considering the complexity of the signaling system, it might seem practical to focus preventive measures to the osteoclasts, which are the final target for all signaling. Recent randomized trials and epidemiological studies suggest that this could bring down the need for later revision surgery (Schilcher et al., 2017).

Taken together, these data show that osteolysis induced by mechanical instability of implants and titanium particles are principally choreographed through the same signaling pathways. Our findings underscore the role of inflammation and innate immune response in aseptic loosening of implants even in the absence of wear debris particles.

Conflict of interest

The authors have no conflicts of interest, financial or otherwise.

Acknowledgments

This study was supported by the Swedish Research Council (K2014-7X-22506-01-3; K2015-99X-10363-23-4), Sweden's Innovation agency (2012-04409) (VINNOVA) and Linköping University. We thank Jenny Welander at Linköping University for her support with GeneSpring.

Appendix A. Supplementary data

Supplementary data to this article can be found online at http://dx.

doi.org/10.1016/j.bonr.2017.07.003.

References

Anthony, P.P., Gie, G.A., Howie, C.R., Ling, R.S., 1990. Localised endosteal bone lysis in relation to the femoral components of cemented total hip arthroplasties. J. Bone Joint Surg. (Br.) 72, 971–979.

Aspenberg, P., Herbertsson, P., 1996. Periprosthetic bone resorption. Particles versus movement. J. Bone Joint Surg. (Br.) 78, 641–646.

Atkins, G.J., Welldon, K.J., Holding, C.A., Haynes, D.R., Howie, D.W., Findlay, D.M., 2009. The induction of a catabolic phenotype in human primary osteoblasts and osteocytes by polyethylene particles. Biomaterials 30, 3672–3681.

Aujla, R.S., Esler, C.N., 2017. Total knee arthroplasty for osteoarthritis in patients less than fifty-five years of age: a systematic review. J. Arthroplast.

Bosetti, M., Masse, A., Navone, R., Cannas, M., 2001. Biochemical and histological evaluation of human synovial-like membrane around failed total hip replacement prostheses during in vitro mechanical loading. J. Mater. Sci. Mater. Med. 12, 693–698.

Burleigh, A., Chanalaris, A., Gardiner, M.D., Driscoll, C., Boruc, O., Saklatvala, J., Vincent, T.L., 2012. Joint immobilization prevents murine osteoarthritis and reveals the highly mechanosensitive nature of protease expression in vivo. Arthritis Rheum. 64, 2278–2288.

Chamoux, E., Houde, N., L'eriger, K., Roux, S., 2008. Osteoprotegerin decreases human osteoclast apoptosis by inhibiting the TRAIL pathway. J. Cell. Physiol. 216, 536–542.

De Benedetti, F., Rucci, N., Del Fattore, A., Peruzzi, B., Paro, R., Longo, M., Vivarelli, M., Muratori, F., Berni, S., Ballanti, P., Ferrari, S., Teti, A., 2006. Impaired skeletal development in interleukin-6-transgenic mice - a model for the impact of chronic inflammation on the growing skeletal system. Arthritis Rheum. 54, 3551–3563.

De Voogd, F.A., Gearry, R.B., Mulder, C.J., Day, A.S., 2016. Osteoprotegerin: a novel biomarker for inflammatory bowel disease and gastrointestinal carcinoma. J. Gastroenterol. Hepatol. 31, 1386–1392.

Fahlgren, A., Bostrom, M.P., Yang, X., Johansson, L., Edlund, U., Agholme, F., Aspenberg, P., 2010. Fluid pressure and flow as a cause of bone resorption. Acta Orthop. 81, 508–516.

Gallo, J., Goodman, S.B., Konttinen, Y.T., Wimmer, M.A., Holinka, M., 2013. Osteolysis around total knee arthroplasty: a review of pathogenetic mechanisms. Acta Biomater. 9, 8046–8058.

Garrigues, G.E., Cho, D.R., Rubash, H.E., Goldring, S.R., Herndon, J.H., Shanbhag, A.S., 2005. Gene expression clustering using self-organizing maps: analysis of the macrophage response to particulate biomaterials. Biomaterials 26, 2933–2945.

Govey, P.M., Kawasawa, Y.I., Donahue, H.J., 2015. Mapping the osteocytic cell response to fluid flow using RNA-Seq. J. Biomech. 48, 4327–4332.

Holen, I., Shipman, C.M., 2006. Role of osteoprotegerin (OPG) in cancer. Clin. Sci. 110, 279–291.

Horowitz, S.M., Gonzales, J.B., 1997. Effects of polyethylene on macrophages. J. Orthop. Res. 15, 50–56.

Ingham, E., Fisher, J., 2005. The role of macrophages in osteolysis of total joint replacement. Biomaterials 26, 1271–1286.

Jones, L.C., Frondoza, C., Hungerford, D.S., 2001. Effect of PMMA particles and movement on an implant interface in a canine model. J. Bone Joint Surg. (Br.) 83, 448–458.

Kadoya, Y., Revell, P.A., Al-Saffar, N., Kobayashi, A., Scott, G., Freeman, M.A., 1996. Bone formation and bone resorption in failed total joint arthroplasties: histomorphometric analysis with histochemical and immunohistochemical technique. J. Orthop. Res. 14, 473–482.

Kim, K.J., Rubash, H.E., Wilson, S.C., D'Antonio, J.A., McClain, E.J., 1993. A histologic and biochemical comparison of the interface tissues in cementless and cemented hip prostheses. Clin. Orthop. Relat. Res. 142–152.

Kim, J.H., Liu, X., Wang, J., Chen, X., Zhang, H., Kim, S.H., Cui, J., Li, R., Zhang, W., Kong, Y., Zhang, J., Shui, W., Lamplot, J., Rogers, M.R., Zhao, C., Wang, N., Rajan, P., Tomal, J., Statz, J., Wu, N., Luu, H.H., Haydon, R.C., He, T.C., 2013. Wnt signaling in bone formation and its therapeutic potential for bone diseases. Ther. Adv. Musculoskelet. Dis. 5, 13–31.

Koulouvaris, P., Ly, K., Ivashkiv, L.B., Bostrom, M.P., Nestor, B.J., Sculco, T.P., Purdue, P.E., 2008. Expression profiling reveals alternative macrophage activation and impaired osteogenesis in periprosthetic osteolysis. J. Orthop. Res. 26, 106–116.

Kurtz, S., Ong, K., Lau, E., Mowat, F., Halpern, M., 2007. Projections of primary and revision hip and knee arthroplasty in the United States from 2005 to 2030. J. Bone Joint Surg. (Am. Vol.) (89a), 780–785.

Liu, C., Zhang, X.Q., Wu, M., You, L.D., 2015. Mechanical loading up-regulates early remodeling signals from osteocytes subjected to physical damage. J. Biomech. 48, 4221–4228.

Lochner, K., Fritsche, A., Jonitz, A., Hansmann, D., Mueller, P., Mueller-Hilke, B., Bader, R., 2011. The potential role of human osteoblasts for periprosthetic osteolysis following exposure to wear particles. Int. J. Mol. Med. 28, 1055–1063.

Maeda, K., Kobayashi, Y., Udagawa, N., Uehara, S., Ishihara, A., Mizoguchi, T., Kikuchi, Y., Takada, I., Kato, S., Kani, S., Nishita, M., Marumo, K., Martin, T.J., Minami, Y., Takahashi, N., 2012. Wnt5a-Ror2 signaling between osteoblast-lineage cells and osteoclast precursors enhances osteoclastogenesis. Nat. Med. 18, 405–412.

McKenzie, J.A., Bixby, E.C., Silva, M.J., 2011. Differential gene expression from microarray analysis distinguishes woven and lamellar bone formation in the rat ulna following mechanical loading. PLoS One 6.

Mi, H., Muruganujan, A., Casagrande, J.T., Thomas, P.D., 2013. Large-scale gene function analysis with the PANTHER classification system. Nat. Protoc. 8, 1551–1566.

Nahidi, L., Leach, S.T., Lemberg, D.A., Day, A.S., 2013. Osteoprotegerin exerts its pro-inflammatory effects through nuclear factor-kappa B activation. Dig. Dis. Sci. 58, 3144–3155.

Nakashima, Y., Sun, D.H., Trindade, M.C., Chun, L.E., Song, Y., Goodman, S.B., Schurman, D.J., Maloney, W.J., Smith, R.L., 1999. Induction of macrophage C-C chemokine expression by titanium alloy and bone cement particles. J. Bone Joint Surg. (Br.) 81, 155–162.

Nich, C., Goodman, S.B., 2014. Role of macrophages in the biological reaction to wear debris from joint replacements. J. Long-Term Eff. Med. Implants 24, 259–265.

Nilsson, A., Norgard, M., Andersson, G., Fahlgren, A., 2012. Fluid pressure induces osteoclast differentiation comparably to titanium particles but through a molecular pathway only partly involving TNFa. J. Cell. Biochem. 113, 1224–1234.

Novack, D.V., Faccio, R., 2011. Osteoclast motility: putting the brakes on bone resorption. Ageing Res. Rev. 10, 54–61.

Okafor, C.C., Haleem-Smith, H., Laqueriere, P., Manner, P.A., Tuan, R.S., 2006. Particulate endocytosis mediates biological responses of human mesenchymal stem cells to titanium wear debris. J. Orthop. Res. 24, 461–473.

Ory, S., Brazier, H., Pawlak, G., Blangy, A., 2008. Rho GTPases in osteoclasts: orchestrators of podosome arrangement. Eur. J. Cell Biol. 87, 469–477.

Pantouli, E., Boehm, M.M., Koka, S., 2005. Inflammatory cytokines activate p38 MAPK to induce osteoprotegerin synthesis by MG-63 cells. Biochem. Biophys. Res. Commun. 329, 224–229.

Queally, J.M., Devitt, B.M., Butler, J.S., Malizia, A.P., Murray, D., Doran, P.P., O'Byrne, J.M., 2009. Cobalt ions induce chemokine secretion in primary human osteoblasts. J. Orthop. Res. 27, 855–864.

Ren, P.G., Irani, A., Huang, Z.N., Ma, T., Biswal, S., Goodman, S.B., 2011. Continuous infusion of UHMWPE particles induces increased bone macrophages and osteolysis. Clin. Orthop. Relat. Res. 469, 113–122.

Reno, C., Marchuk, L., Sciore, P., Frank, C.B., Hart, D.A., 1997. Rapid isolation of total RNA from small samples of hypocellular, dense connective tissues. Biotechniques 22, 1082–1086.

Robertsson, O., Wingstrand, H., Kesteris, U., Jonsson, K., Onnerfalt, R., 1997. Intracapsular pressure and loosening of hip prostheses. Preoperative measurements in 18 hips. Acta Orthop. Scand. 68, 231–234.

Sabokbar, A., Rushton, N., 1995. Role of inflammatory mediators and adhesion molecules in the pathogenesis of aseptic loosening in total hip arthroplasties. J. Arthroplast. 10, 810–816.

Schilcher, J., Palm, L., Ivarsson, I., Aspenberg, P., 2017. Local bisphosphonate reduces migration and formation of radiolucent lines adjacent to cemented acetabular components. Bone Joint J. 99-B, 317–324.

Sims, N.A., Walsh, N.C., 2010. GP130 cytokines and bone remodelling in health and disease. BMB Rep. 43, 513–523.

Skoglund, B., Aspenberg, P., 2003. PMMA particles and pressure—a study of the osteolytic properties of two agents proposed to cause prosthetic loosening. J. Orthop. Res. 21, 196–201.

Skripitz, R., Aspenberg, P., 2000. Pressure-induced periprosthetic osteolysis: a rat model. J. Orthop. Res. 18, 481–484.

Stadelmann, V.A., Terrier, A., Pioletti, D.P., 2008. Microstimulation at the bone-implant interface upregulates osteoclast activation pathways. Bone 42, 358–364.

Sundfeldt, M., Carlsson, L.V., Johansson, C.B., Thomsen, P., Gretzer, C., 2006. Aseptic loosening, not only a question of wear: a review of different theories. Acta Orthop. 77, 177–197.

Tomankova, T., Kriegova, E., Fillerova, R., Luzna, P., Ehrmann, J., Gallo, J., 2014. Comparison of periprosthetic tissues in knee and hip joints: differential expression of CCL3 and DC-STAMP in total knee and hip arthroplasty and similar cytokine profiles in primary knee and hip osteoarthritis. Osteoarthr. Cartil. 22, 1851–1860.

Ulrich, S.D., Seyler, T.M., Bennett, D., Delanois, R.E., Saleh, K.J., Thongtrangan, I., Kuskowski, M., Cheng, E.Y., Sharkey, P.F., Parvizi, J., Stiehl, J.B., Mont, M.A., 2008. Total hip arthroplasties: what are the reasons for revision? Int. Orthop. 32, 597–604.

Van der Vis, H.M., Aspenberg, P., Tigchelaar, W., Van Noorden, C.J., 1999. Mechanical compression of a fibrous membrane surrounding bone causes bone resorption. Acta Histochem. 101, 203–212.

Veronesi, F., Tschon, M., Fini, M., 2017. Gene expression in osteolysis: review on the identification of altered molecular pathways in preclinical and clinical studies. Int. J. Mol. Sci. 18.

van der Vis, H.M., Aspenberg, P., de Kleine, R., Tigchelaar, W., van Noorden, C.J.F., 1998. Short periods of oscillating fluid pressure directed at a titanium-bone interface in rabbits lead to bone lysis. Acta Orthop. Scand. 69, 5–10.

Walter, W.L., Walter, W.K., O'Sullivan, M., 2004. The pumping of fluid in cementless cups with holes. J. Arthroplast. 19, 230–234.

Wang, M.L., Nesti, L.J., Tuli, R., Lazatin, J., Danielson, K.G., Sharkey, P.F., Tuan, R.S., 2002. Titanium particles suppress expression of osteoblastic phenotype in human mesenchymal stem cells. J. Orthop. Res. 20, 1175–1184.

Wang, C.T., Lin, Y.T., Chiang, B.L., Lee, S.S., Hou, S.M., 2010. Over-expression of receptor activator of nuclear factor-kappa B ligand (RANKL), inflammatory cytokines, and chemokines in periprosthetic osteolysis of loosened total hip arthroplasty. Biomaterials 31, 77–82.

Wei, W., Zeve, D., Suh, J.M., Wang, X.Q., Du, Y., Zerwekh, J.E., Dechow, P.C., Graff, J.M., Wan, Y.H., 2011. Biphasic and dosage-dependent regulation of osteoclastogenesis by beta-catenin. Mol. Cell. Biol. 31, 4706–4719.

Weinstein, R.S., O'Brien, C.A., Almeida, M., Zhao, H.B., Roberson, P.K., Jilka, R.L., Manolagas, S.C., 2011. Osteoprotegerin prevents glucocorticoid-induced osteocyte apoptosis in mice. Endocrinology 152, 3323–3331.

Weivoda, M.M., Ruan, M., Hachfeld, C.M., Pederson, L., Howe, A., Davey, R.A., Zajac, J.D., Kobayashi, Y., Williams, B.O., Westendorf, J.J., Khosla, S., Oursler, M.J., 2016. Wnt signaling inhibits osteoclast differentiation by activating canonical and non-canonical cAMP/PKA pathways. J. Bone Miner. Res. 31 (1), 65–75. http://dx.doi.org/10.1002/jbmr.2599. Epub 2015 Aug 19.

Westendorf, J.J., Kahler, R.A., Schroeder, T.M., 2004. Wnt signaling in osteoblasts and bone diseases. Gene 341, 19–39.

Xu, J.W., Konttinen, Y.T., Lassus, J., Natah, S., Ceponis, A., Solovieva, S., Aspenberg, P., Santavirta, S., 1996. Tumor necrosis factor-alpha (TNF-alpha) in loosening of total hip replacement (THR). Clin. Exp. Rheumatol. 14, 643–648.

Yang, G.G., Im, H.J., Wang, J.H.C., 2005. Repetitive mechanical stretching modulates IL-1 beta induced COX-2, MMP-1 expression, and PGE(2) production in human patellar tendon fibroblasts. Gene 363, 166–172.